Journal Pre-proofs

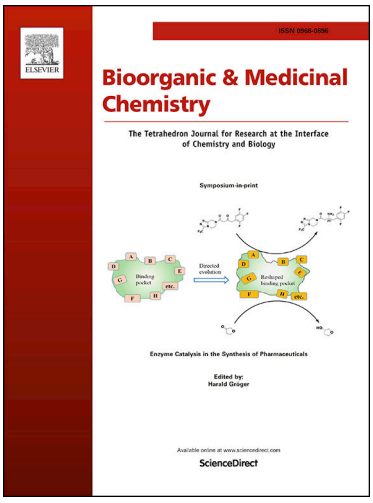

Exploring the physicochemical and antiproliferative properties of biaryl-linked [13]-macrodilactones

Chengsheng Chen, Cristin Bosko, Catherine McGeough, Ryan McLean, Angela M. Zaino, M. Kyle Hadden, Mark W. Peczuh

PII: S0968-0896(20)30501-0
DOI: https://doi.org/10.1016/j.bmc.2020.115671
Reference: BMC 115671

To appear in: *Bioorganic & Medicinal Chemistry*

Received Date: 26 November 2019
Revised Date: 20 July 2020
Accepted Date: 22 July 2020

Please cite this article as: C. Chen, C. Bosko, C. McGeough, R. McLean, A.M. Zaino, M. Kyle Hadden, M.W. Peczuh, Exploring the physicochemical and antiproliferative properties of biaryl-linked [13]-macrodilactones, *Bioorganic & Medicinal Chemistry* (2020), doi: https://doi.org/10.1016/j.bmc.2020.115671

Graphical Abstract

To create your abstract, type over the instructions in the template box below.
Fonts or abstract dimensions should not be changed or altered.

Exploring the physicochemical and antiproliferative properties of biaryl-linked [13]-macrodilactones

Leave this area blank for abstract info.

Chengsheng Chen, Cristin Bosko, Catherine McGeough, Ryan McLean, Angela M. Zaino, M. Kyle Hadden, Mark W. Peczuh

Department of Chemistry, University of Connecticut, 55 N. Eagleville Road U3060, Storrs, CT

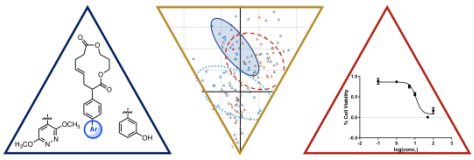

ELSEVIER

Bioorganic & Medicinal Chemistry
journal homepage: www.elsevier.com

Exploring the physicochemical and antiproliferative properties of biaryl-linked [13]-macrodilactones

Chengsheng Chen,[a] Cristin Bosko,[a] Catherine McGeough,[a] Ryan McLean,[a] Angela M. Zaino,[b] M. Kyle Hadden,[b] Mark W. Peczuh[a]*

[a] *Department of Chemistry, University of Connecticut, 55 N. Eagleville Road U3060, Storrs, CT*
[b] *Department of Pharmaceutical Sciences, School of Pharmacy, 69 N. Eagleville Road U3092, University of Connecticut, Storrs, Connecticut 06269*

ARTICLE INFO

Article history:
Received
Received in revised form
Accepted
Available online

Keywords:
macrocycle
principle component analysis
synthesis
antiproliferative

ABSTRACT

A macrocyclic motif fosters productive protein-small molecule interactions. There are numerous examples of both natural product and designed, synthetic macrocycles that modulate the immune system, slow microbial infection, or kill eukaryotic cells. Reported here are the synthesis, physicochemical characterization, and antiproliferative activity of a group of [13]-macrodilactones decorated with a pendant biaryl moiety. Biaryl analogs were prepared by Suzuki reactions conducted on a common intermediate that contained a bromophenyl unit alpha to one of the carbonyls of the [13]-macrodilactone. Principal component analysis placed the new compounds in physicochemical context relative to a variety of pharmaceuticals and natural products. Modest inhibition of proliferation was observed in ASZ cells, a murine basal cell carcinoma line. This work underscores the value of an approach toward the identification of bioactive compounds that places the evaluation of physicochemical parameters early in the search process.

1. Introduction

Macrocycles hold potential as drug candidates and as tool compounds in chemical biology applications.[1,2,3,4] Their properties, particularly their size, fill a gap between small molecules and proteins with respect to bioactive molecules. Macrocycles can take up shapes that mimic protein secondary structural motifs such as alpha-helices and beta-turns, making them candidates for the inhibition of deleterious protein-protein interactions.[5] Compared to acyclic molecules of similar molecular weight, the reduced flexibility of macrocycles improves selectivity in binding to a biological target.[6] This rigidification results in a certain shape that is associated with a specific macrocyclic backbone; the shape is largely dictated by the number of atoms in the ring, the hybridization of ring atoms, and stereogenic centers. Additional features then allow for local flexibility within a motif. By understanding the factors that influence the topology of a macrocycle, they can then be applied to the preparation of new compounds with designed properties.

Our group is investigating the synthesis, structural and physical properties, and biological activity of a class of [13]-macrodilactones that contain an uncommon element of stereogenicity as a key structural feature.[7,8,9,10,11] Based on the number of atoms in the ring, their organization into planar units, and their relationship to each other, the double bond of the alkene orients itself perpendicular to the mean plane of the macrocycle. This gives rise to a stereogenic axis – in contrast to a stereogenic center. A planar chirality is therefore associated with the macrocycles. In a previous report, we described the synthesis, anti-migratory, and anti-proliferative activity of a group of lipid-linked [13]-macrodilactones, of which **1**-**3** (Fig. 1) were examples.[12] The study was inspired by simple macrocycles such as the natural product migrastatin and related de novo macrocycles that had been shown to slow the migration of mammalian cancer cells.[13,14] We found that **1**-**3** had similar antimigratory activities against BT-20 breast cancer cells (≤75 μM IC_{50}), but **1** and **2** were cytostatic and **3** was cytotoxic at 100 μM.

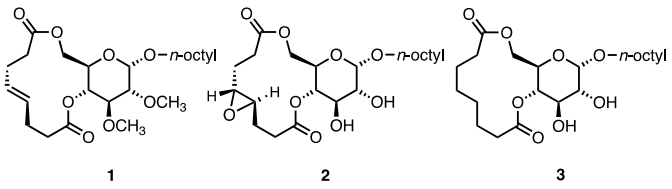

Figure 1. Previously investigated cytotoxic, lipid-linked [13]-macrodilactones **1**, **2**, and **3**.

We became interested in having a way to modulate the identity and subsequent properties of the hydrophobic portion of

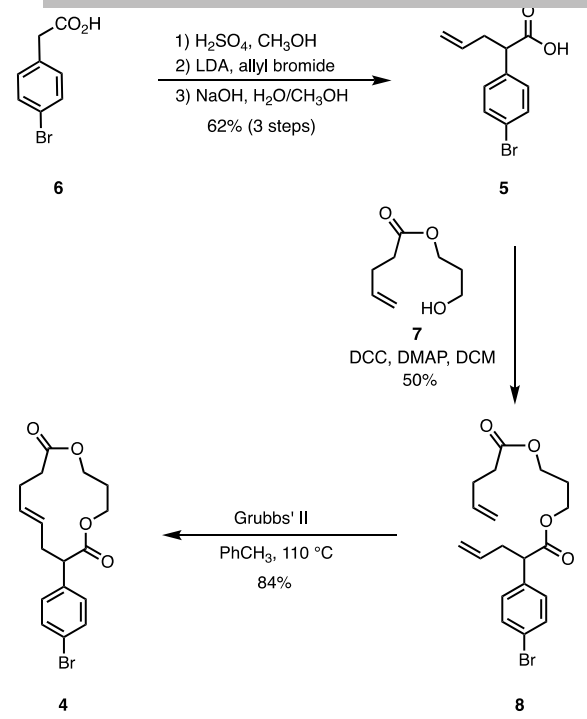

Scheme 1. Synthesis of [13]-Macrodilactone **4**.

the molecule while maintaining the planar chiral feature of the [13]-macrodilactone. Here we describe one approach toward addressing that goal via the synthesis of new biaryl-linked [13]-macrodilactones, their principle component analysis (PCA), and anti-proliferation assays. Important considerations that led us toward this family of macrocycles were three-fold. First, we wanted to put the moiety at a key stereogenic carbon that would work in concert with the ribbon-like shape of the macrocycle. Second, we wanted to probe a part of the macrocyclic backbone that was different than in compounds **1**-**3**. Third, we sought a structure and synthetic strategy that was amenable to the preparation of several analogs.

2. Results and Discussion

2.1. Synthesis of [13]-macrodilactones

At the outset, our intention was to prepare a [13]-macrodilactone containing a pendant group that was poised for diversification via a straightforward chemoselective reaction, in this case a Suzuki coupling. An aryl halide, attached at a position alpha to the ester carbonyl, would enable us to implement such a plan. The alpha-(*p*-bromophenyl) [13]-macrodilactone **4** was therefore prepared by a strategy that leveraged our previous experience with the synthesis of these macrocycles (Scheme 1).[7] We have shown that 1,3-propane diol and related 1,3-diols can be sequentially acylated with different pentenoic acids to give diacyl diesters that ultimately yield to ring closing metathesis (RCM) using ruthenium-based metathesis catalysts.[15] In the present work, our strategy made use of 2-(*p*-bromophenyl)-4-pentenoic acid **5** as the key acylating agent. Compound **5** was itself prepared from commercially available 4-bromophenyl acetic acid **6** via esterification, alkylation, and hydrolysis (62 % over three steps).[16,17] Substituted pentenoic acid **5** was then esterified using the mono-acyl alcohol **7** under the action of DCC and DMAP to deliver diacyl-diene **8** in 50% yield.[8] RCM on diene **8** afforded C7-(*p*-bromophenyl)-[13]-macrodilactone **4** (84%). Having established access to **4**, the stage was now set for its derivatization via Suzuki coupling reactions. Suzuki cross couplings were conducted to convert the pendant aryl bromide into a variety of biaryls attached to the [13]-macrodilactone scaffold. A common set of reaction conditions was identified that were able to deliver the product macrocycles with yields sufficient for their further characterization (Table 1).[18] Macrocycles containing biaryl moieties that were strictly hydrophobic (i.e. **10a**, **10b**), or that incorporated heteroatoms into the biaryl unit in one way or the other (i.e, **10c**-**10k**) were prepared. Aryl units containing heteroatoms were introduced to increase the polarity of the hydrophobic macrocycles and potentially enable them to permeate through cell membranes via active uptake mechanisms.

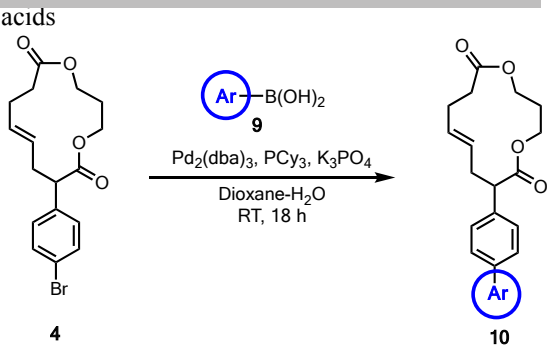

entry	Ar	Ar-$B(OH)_2$	Product	Yield (%)	GI_{50}[a] (μM)
1	phenyl	**9a**	**10a**	77	≥100
2	mesityl	**9b**	**10b**	47	N/A[b]
3	3-OH-phenyl	**9c**	**10c**	52	12.1±0.5
4	3-N$(CH_3)_2$-phenyl	**9d**	**10d**	61	≥75
5	*m*-pyridyl	**9e**	**10e**	83	40.9±0.3
6	*p*-pyridyl	**9f**	**10f**	56	≥75
7	pyrimidyl	**9g**	**10g**	93	N/A
8	5-(3,6-dimethoxy-pyridazine)	**9h**	**10h**	98	19.7±4.4
9	4-indoylyl	**9i**	**10i**	61	N/A
10	4-(3,5-dimethyl-isoxazole)	**9j**	**10j**	73	≥75
11	4-(1-benzyl-pyrazolyl)	**9k**	**10k**	76	≥100

[a] GI_{50} values are the avg ± SEM of two separate experiments, run in triplicate.

[b] N/A = insufficient data to determine GI_{50}; data not available.

2.2. Antiproliferation assays

Cell viability assays were conducted using the ASZ cell line to evaluate the cytotoxicity of the new [13]-macrodilactones. The ASZ line is a mouse-derived, basal cell carcinoma cell line that is easy to manage in cell culture and replicates at an appreciable rate, making it a useful model to evaluate the compounds in the project. We had previously measured cell viability using BT-20 cells, a human breast cancer cell line, but opted here to use the ASZ cells for convenience; both cell lines are suitable for cell viability assays. The MTS/PMS assay used, quantifies cell viability in comparison to cells treated with DMSO by the reduction of tetrazolium salts which results in the formation of

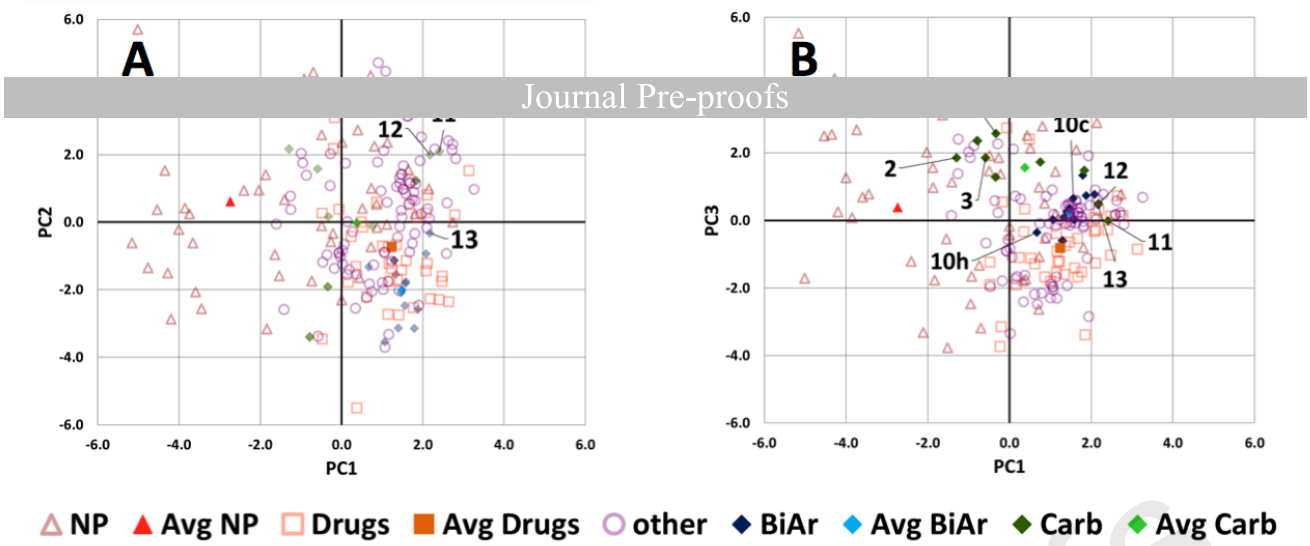

Figure 2. PCA. A library of 208 compounds was broken into sets: natural products (NP), drugs, other, biaryl [13]-macrodilactones **10a-10k** (biAr), carbohydrate-fused [13]-macrodilactones like **1-3** (carb), and reference compounds **11-13**. **A.** PC1 vs PC2 **B.** PC1 vs PC3

Figure 3. [13]-Macrodilactones **11**, **12**, and **13** shown in Figure 2 and described in the text.

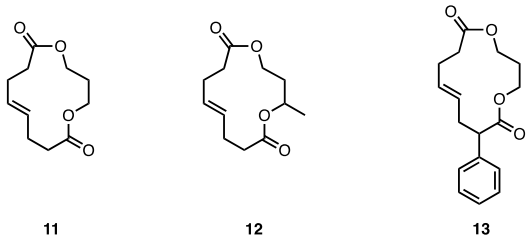

11 12 13

formazan dyes which can be quantified by absorbance at ~490 nm.[19,20] Using MTS and PMS over other tetrazolium dyes such as MTT or XTT provides rapid color development, stable reagents in solution, and aqueously soluble formazan products. [21]

The effect on ASZ cell viability of compounds (**10a-10k**) was tested at concentrations ranging from 100 - 0.1 μM, to provide a dose response curve for the compounds. As shown in Table 1, several of the new [13]-macrodilactones possessed anti-proliferative activity. Potency in the assay was used to divide the compounds into four groups. Compounds **10c** and **10h** possessed the greatest antiproliferative activity, with GI_{50} values of 12.1 and 19.7 μM, respectively. Compound **10e** showed intermediate anti-proliferative activity, whereas compounds **10d**, **10f**, and **10j** showed only slight changes in cell viability. The final cohort of compounds **10a** and **10k** showed no activity or change in cell viability in comparison to treatment with DMSO. Notably, the potency of compounds **10c** and **10h** was similar to that of the carbohydrate-fused, lipid-functionalized macrocycles (i.e., **1-3**) that we had previously studied. Moreover, the fact that there was a range of activities amongst this family of compounds prompted us to revisit the physicochemical properties of the compounds.

2.3. Physicochemical characterization

We next endeavored to find out where, in chemical space, the new biaryl set of [13]-macrodilactones (biAr) resided. Principal component analysis (PCA) was performed on the biAr compounds in order to compare their properties to a diverse collection of natural products (NP), currently available drugs (drug), drug-like and natural product-like compounds, including macrocycles described by Tan and co-workers (other),[22] and the carbohydrate fused [13]-macrodilactones we had investigated previously (carb). To that end, we adopted a method for PCA established by Tan and co-workers.[23] Their collection of reference compounds was comprised of drugs, natural products, and drug-like library members, in addition to some additional macrocycles to form a library of over 180 compounds used in the analysis.[22,23] Once the entire library of compounds was assembled, twenty structural and physiochemical parameters were collected for them, and the data was then normalized so that it could be exported to a statistical program in order to calculate the principal components (PCs). The number of PCs obtained was equal to the number of parameters used so in this case there were twenty PCs; only the first three were used to generate the PCA plots (Fig. 2) because together they expressed ≥75% of the variance present in the original data. As we set about analyzing the plots, we were cognizant that over-analysis of the PCA would add little additional value to the study.[22]

Inspection of the PCA plots led to observations on the general characteristics of the compound sets in the library. In the PC1 vs PC2 plot (Fig 2A),[24] compounds of the NP set were spread across a crescent-shaped space. In the PC1 vs PC3 plot (Fig 2B), NPs were distributed more widely. The shape defined by the set likely reflected the broad range of molecular weights, along with contributions from other parameters of NPs. The drug set was mostly localized in one octant of the chemical space and largely separate from the NP set, especially with respect to the PC1 vs PC2 plot. Differences in how natural products and drugs occupy their respective chemical spaces may be attributable to the fact that natural products typically have more rotatable bonds and more stereogenic centers along with higher molecular weights.[25] The "other" compounds set further enriched the chemical space; it shared some overlap with drugs as shown in the PC1 vs PC2 plot, while also extending beyond it to occupy some unique space (i.e., upper right quadrants). Unlike drugs, the other set contains both biologically active and inactive compounds, which may reflect the fact that they have not been selected for by parameters related to bioavailability.[26] Overall, the NP, drug, and other sets occupied relatively distinct chemical spaces in the PCA. The plots also contain simulated spots that represent virtual compounds composed from the average values of each defined set, and the NP average spot is distant from the average drug spot, and underscores the differences present between these two sets of compounds. The reasoning for this difference and the deeper meaning behind the location of the spots in chemical

spac ame the principal components.

We gleaned information about which parameters contributed to the variance in the principal components from the loading plots and the coefficients of each of the parameters in the PCA (See Supplementary data). Loading plots provided a useful qualitative view on how specific parameters affect the location of a compound on the PCA plots. Further, the coefficients from which the loading plots were built provided a quantitative understating of which parameters had the greatest effect on the PCA plots. Parameters such as H-bond acceptors (HBA), topological polar surface area (tPSA) and the number of oxygen atoms (O) had the greatest effect on PC1. For PC2, aromatic ring count (RingAr), hydrophobicity (ALOGPs), and aqueous solubility (ALOGpS) were key, and the number of nitrogen atoms (N) was a major component of PC3. Depending on the sign (+/-), these parameters could move in one direction or the other with respect to a given PC. Consideration of individual parameters within the PCs, as listed above, provided insight into molecular characteristics of the compound sets we defined. By considering the three PCs together it was determined that the following parameters are key to the entire PCA due their significance in more than one of the PCs: sp^3 -hybridized carbons (Fsp^3), relative polar surface area (relPSA), ALOGPs, aqueous solubility (LogD and ALOGpS), and RingsAr (See table in the Supplementary data). This enables a better understanding of how the PCA plot as a whole 3D-space was affected by the parameters. Our evaluation of these parameters is comparable to that of Tan *et al.* who obtained similar results using the same base library to evaluate their compounds. The only major difference between our results and theirs is the importance RingsAr, which is in line with the fact that compounds like **10a-10k** that we report here incorporate a biaryl moiety as a key structural feature.

Three [13]-macrodilactones from our library – unfunctionalized macrocycle **11** and the C2-methyl and C7-phenyl macrocycles **12** and **13**, respectively (Fig. 3) – illustrate the practical effects of RingsAr and Fsp^3 by illustrating how these structures related to each other on the plots. This effect is clearly seen in the PC1 vs PC2 plot (Fig. 2A), which makes sense due to the fact that both parameters contriubte significantly to PC2. In the plot, phenyl substituted macrocycle **13** is located in the lower right quadrant, underneath the other two compounds, which coincides with the downward influence of RingsAr (See loading plot in the Supplementary data). Similarly, methyl substituted macrocycle **12** resides to the left of the unfunctionalized ring **11**, which is in agreement with the influence of Fsp^3.

By evaluating the distributions in the PCA plots of the new biaryl-functionalized [13]-macrodilactones (**10a-10k**, biAr) and their carbohydrate-fused counterparts (e.g., **1-3**, carb), valuable insights about the differences between them became apparent. Both sets contain the [13]-macrodilactone (i.e., **11**) core in common. The synthetic approach used to access them is modular in nature and allows for broad functionalization. Consequently, differences arise from the details (i.e., diversification strategy or starting materials) in the preparation of each set. The biAr set relied on late-stage functionalization via Suzuki reactions, whereas the carb set used pyranose sugars to template the core of the [13]-macrodilactone. In general, the biAr [13]-macrodilactones (**10a-10k**) occupy chemical space that overlaps with compounds in the drug set of the library (Fig 2B). These compounds also occupy a much smaller area of chemical space in comparison to the carb set. This is due to the factors discussed suggests, all of the compounds in the biAr set contain a biaryl system due to the Suzuki coupling. Compounds in the carb set (e.g., **1-3**), on the other hand, tend to be more natural product-like, based on their distribution in the PCA plots. This is caused by two main factors. First, these compounds have more heteroatoms, specifically oxygen atoms, from the sugar that has been incorporated into the macrocyclic structure. Second, the Fsp^3 is higher due to both the carbohydrate ring and the alkyl chain in octyl glycosides.

The chemical space that both sets cover is relatively broad, and the carb set occupies more overall PC space than does the biAr set. In the PC1 vs PC2 plot, for example (Fig. 2A), most compounds in the biAr sets reside in the lower right part of the plot along with most drug compounds, while the carb set starts in the lower right and spreads out into the upper left quadrant, showing little separation between the sets. The clearest distinction between these two sets can been seen in the PC1 vs PC3 plot (Fig. 2B) where the biAr set is localized mostly in the upper right quadrant just above the x-axis while the carb set is in the upper left quadrant. In general, the biAr set tracks towards drugs and the carb set tracks toward NPs. The PCA, therefore, makes sense with respect to the overall nature of these two sets of [13]-macrodilactones. That is, appending heterobiaryl groups to the macrocycle makes their properties more drug-like, while a fused carbohydrate makes their properties more natural product-like. Both sets of derivatives maintain a common [13]-macrodilactone core but nonetheless occupy somewhat complementary areas of chemical space. Further, the fact that specific compounds (i.e., **1-3** and **10c**, **10h**) in each of the sets were antiproliferative suggests that activity can be maintained despite these slight variations in structure.

3. Conclusion

In conclusion, we have synthesized a new class of C7-substituted [13]-macrodilactones, using a Suzuki coupling as the key, late-stage diversifying reaction. Principal component analysis (PCA) was a valuable tool for characterizing the new compounds in physicochemical space. PCA allowed the new biaryl [13]-macrodilactones (**10**) to be placed in the context of natural products, drugs and other compounds, and the carbohydrate-fused [13]-macrodilactones (e.g., **1-3**) that were studied previously. Further, individual compounds in the set (i.e., **10c** and **10h**) showed anti-proliferative activity of similar potency to **1-3**. The modest antiproliferative effect of the [13]-macrodilactones reported here motivates the incorporation of their structural and physicochemical features into the design of related families of macrocycles.

Moreover, this investigation reported here suggests that, by determining which parameters are of key interest, PCA may help guide synthetic planning of sets of compounds. For example, incorporation of stereogenic centers may tilt a set of compounds toward greater natural product-like character. Alternatively, the addition of hetero-biaryl units may make a scaffold more drug-like. It is notable that the depsipeptide macrocycle Teixobactin contains a polar ring connected to a pendant peptide containing hydrophobic amino acids.[27] The Teixobactin structure is loosely related to our [13]-macrodilactones and suggests additional motifs that can be explored.

4. Experimental

4.1. Synthetic Procedures

4.1.1. 2-(p-Bromophenyl)-4-pentenoic acid ***5***[17]

(1.00 g, 4.65 mmol) in methanol (50 mL) at 0 °C, was slowly added H_2SO_4 (5 mL). The mixture was heated under reflux for 3 hours and then allowed to cool to room temperature and diluted with ethyl acetate (350 mL). The solution was washed with water (3 x 60 mL), and the organic layer was dried over Na_2SO_4 and concentrated under reduced pressure to give the methyl ester in 90% yield as a pale-yellow oil. ^{1}H NMR ($CDCl_3$) 300 MHz: δ 7.43 (d, J = 8.4 Hz, 2H), 7.14 (d, J = 8.4 Hz, 2H), 3.67 (s, 3H), 3.56 (s, 2H). ^{13}C NMR ($CDCl_3$) 75 MHz: δ 171.4, 133.0, 131.6, 131.0, 121.1, 52.1, 40.5. Alkylation. In a flame dried 100 mL round bottomed flask, diisopropylamine (4.18 mmol, 0.59 mL) was dissolved in 20 mL dry THF. The solution was cooled to -78 °C under N2 and n-butylllithium (2.7 mL, 4.39 mmol, 1.6 M in hexanes) was added dropwise over 10 min. After stirring for an additional 30 min, methyl 4-bromophenylacetate (0.96 g, 4.18 mmol) in 3 mL THF was quickly added to the LDA solution. The reaction was maintained at -78 °C for 30 min, and then allyl bromide (0.39 mL, 4.56 mmol) was added dropwise to the reaction mixture. The reaction was stirred and allow to warm to room temperature over 2 hours. The solution was then diluted with ethyl acetate (40 mL) and washed with saturated NH4Cl solution (1 x 20 mL). The organic layer was dried over Na_2SO_4 and the solvent was removed under reduced pressure. The residue was purified by silica gel column chromatography to give the alkylated ester as a light-yellow oil in 72% yield. Rf 0.6 (10% EtOAc/Hex). ^{1}H NMR ($CDCl_3$) 300 MHz: δ 7.45 (d, J = 8.5 Hz, 2H), 7.20 (d, J = 8.4 Hz, 2H), 5.70 (dddd, J = 17.0, 10.2, 6.8, 6.8 Hz, 1H), 5.18–4.93 (m, 2H), 3.66 (s, 3H), 3.63 (dd, J = 19.5, 9.7 Hz, 1H), 2.81 (ddd, J = 14.3, 7.1, 7.1 Hz, 1H), 2.50 (ddd, J = 14.0, 6.9, 6.9 Hz, 1H). ^{13}C NMR ($CDCl_3$) 75 MHz: δ 173.4, 137.4, 134.8, 131.7, 129.7, 121.3, 117.4, 52.1, 50.8, 37.4. Hydrolysis. The alkylated ester (0.81 g, 3.01 mmol) was dissolved in a mixture of water and methanol (3:1, 12 mL). Sodium hydroxide (0.16 g, 3.91 mmol) was then added as a solid in one portion and the mixture was and stirred overnight at room temperature. After, the reaction was acidified by addition of 1M HCl to pH 1 and then extracted with ethyl acetate (3 x 20 mL). The combined extracts were dried over Na_2SO_4, filtered, and the solvent was removed under reduced pressure. Pure pentenoic acid 4 was obtained as a yellow oil in quantitative yield and was used without additional purification. ^{1}H NMR ($CDCl_3$) 400 MHz: δ 11.74 (s,br, 1H), 7.47 (d, J = 8.4 Hz, 2H), 7.22 (d, J = 8.5 Hz, 2H), 5.71 (dddd, J = 17.0, 10.2, 6.8, 6.8 Hz, 1H), 5.15–5.02 (m, 2H), 3.64 (dd, J = 14.6, 6.9 Hz, 1H), 2.82 (ddd, J = 14.5, 7.1, 7.1 Hz, 1H), 2.53 (ddd, J = 14.2, 7.0, 7.0 Hz , 1H). ^{13}C NMR ($CDCl_3$) 100 MHz: δ 179.6, 136.8, 134.5, 131.9, 129.9, 121.8, 117.8, 50.9, 37.0.

4.1.2. 3-hydroxypropyl 4-pentenoate (7)[8]

Dicyclohexylcarbodiimide (DCC) (1.34 g, 6.48 mmol) and N,N-dimethylaminopyridine (DMAP) (366.5 mg, 3.00 mmol) were dissolved in DCM (45 mL), and the solution was cooled to 0 °C on an ice bath. 4-Pentenoic acid (600.7 mg, 6.00 mmol) was added and the mixture was stirred at the same temperature for 30 min. Then, 1,3-propanediol (456.5 mg, 6.00 mmol) in DCM (5 mL) was added to the mixture which was stirred overnight at room temperature. The reaction mixture was then filtered through a short pad of Celite, the solvent was removed from the filtrate under reduced pressure, and the residue was purified by silica gel column chromatography to give **7** as a colorless oil (455 mg, 48% yield). Rf 0.17 (20% EtOAc/Hex). ^{1}H NMR ($CDCl_3$) 300 MHz: δ 5.70 (dddd, J = 16.6, 10.3, 6.2, 6.2 Hz, 1H), 5.01–4.83 (m, 2H), 4.10 (t, J = 6.4 Hz, 2H), 3.56 (t, J = 6.2 Hz, 2H), 3.18 (s, 1H), 2.37–2.17 (m, 4H), 1.75 (p, J = 6.3 Hz, 2H). ^{13}C NMR 28.6.

4.1.3. Compound 8[7]

DCC (647.3 mg, 3.14 mmol) and DMAP (174.2 mg, 1.43 mmol) were dissolved in DCM (12 mL), and the solution was cooled to 0 °C. 2-(*p*-Bromophenyl)-4-pentenoic acid **5** (800.0 mg, 3.14 mmol) was added and the mixture was stirred at the same temperature for 30 min. Then, 3-hydroxypropyl 4-pentenoate **7** (450.6 mg, 2.85 mmol) in DCM (1 mL) was then added to the mixture and it was stirred at room temperature overnight. After, the mixture was filtered through a short pad of Celite and the solvent was removed from the filtrate under reduced pressure. The residue was purified by silica gel column chromatography to give diene **8** as a colorless oil (563 mg, 50% yield). Rf 0.44 (10% EtOAc/Hex). ^{1}H NMR ($CDCl_3$) 300 MHz: δ 7.41 (d, J = 8.4 Hz, 2H), 7.15 (d, J = 8.4 Hz, 2H) , 5.83-5.59 (m, 2H), 5.10–4.91 (m, 4H), 4.11 (q, J = 6.3 Hz, 2H), 4.04 (t, J = 6.3 Hz, 2H), 3.58 (dd, J = 8.4, 7.1 Hz, 1H), 2.76 (ddd, J = 14.5, 7.4, 7.4 Hz, 1H), 2.46 (ddd, J = 13.9, 6.8, 6.8 Hz, 1H), 2.40–2.27 (m, 4H), 1.88 (p, J = 6.4 Hz, 2H). ^{13}C NMR ($CDCl_3$) 75 MHz: δ 172.7, 137.4, 136.5, 134.7, 131.7, 129.6, 121.3, 117.4, 115.5, 61.4, 60.7, 50.8, 37.3, 33.4, 28.8, 27.9. TOF HRMS: m/z calcd for $C_{19}H_{24}O_4Br$ [M+H]+: 395.0858; found: 395.0845.

4.1.4. [13]-Macrodilactone 4[7]

Grubbs' second-generation catalyst (60.2 mg, 0.071 mmol) was added as a solid in one portion to a solution of diene **8** (560 mg, 1.42 mmol) in toluene (200 mL). The mixture was heated to reflux overnight (18 h). The mixture was then allowed to cool to room temperature, and then the toluene was removed under reduced pressure and the crude product was purified by silica gel column chromatography to give [13]-macrodilactone **4** as a white solid (438 mg, 84% yield). mp 108.8– 111.0 °C. Rf 0.45 (20% EtOAc/Hex). ^{1}H NMR ($CDCl_3$) 300 MHz: δ 7.45 (d, J = 8.4 Hz, 1H), 7.27 (d, J = 8.4 Hz, 1H), 5.66–5.44 (m, 2H), 4.59-4.40 (m, 2H), 4.03 (dt, J = 11.2, 4.2 Hz, 1H), 3.86 (dt, J = 11.2, 4.1 Hz, 1H), 3.57 (dd, J = 12.4, 2.9 Hz, 1H), 2.73 (ddd, J = 12.9, 12.9, 8.1 Hz, 1H), 2.52–2.22 (m, 5H), 2.10-1.99 (m, 2H). ^{13}C NMR ($CDCl_3$) 75 MHz: δ 173.7, 137.9, 131.8, 131.3, 129.5, 128.5, 121.5, 60.7, 60.2, 51.4, 37.8, 34.1, 28.6, 25.8. TOF HRMS: m/z calcd for $C_{17}H_{20}O_4Br$ [M+H]+: 367.0545; found: 367.0545.

4.1.5. General procedure for Suzuki reactions on [13]-macrodilactone 4

The (hetero)aryl boronic acid (0.15 mmol), [Pd_2-$(dba)_3$] (1.3 mg, 0.0012 mmol), PCy3 (0.9 mg, 0.0033 mmol) and the [13]-macrodilactone **4** (50 mg, 0.136 mmol) were added to a 5 mL vial equipped with a stir bar under nitrogen. The vial was sealed, evacuated and refilled with nitrogen for ten minutes. Dioxane (0.7 mL), and aqueous K_3PO_4 (0.5 mg, 0.23 mmol in 0.18 ml H_2O) were added by syringe. The vial was heated at 100 ºC for 18 h with vigorous stirring. The mixture was allowed to cool to room temperature and then filtered through a pad of silica gel with washing by EtOAc. The filtrate was dried over anhydrous Na_2SO_4 and then concentrated. The residue was purified by column chromatography on silica gel using hexanes:ethyl acetate solutions as reported for each compound.

4.1.5.1. Compound 10a

This compound was prepared by using the general procedure for Suzuki reactions with compound **9a** to give compound **10a** as a white solid (38 mg, 77% yield). mp 126.1-127.0 °C. Rf 0.64 (15% EtOAc/Hex). ^{1}H NMR ($CDCl_3$) 400 MHz: δ 7.56 (td, J = 7.2, 6.5, 1.8 Hz, 4H), 7.50–7.39 (m, 4H), 7.37–7.30 (m, 1H), 5.66–5.49 (m, 2H), 4.57 (ddd, J = 11.1, 8.2, 6.6 Hz, 1H), 4.51–4.39 (m, 1H), 4.03 (dt, J = 11.2, 4.2 Hz, 1H), 3.87 (dt, J = 11.2,

4.1 [illegible] 0.3, 13.0, 8.1 Hz, 1H), 2.48–2.28 (m, 5H), 2.10–1.99 (m, 2H). ^{13}C NMR ($CDCl_3$) 100 MHz: δ 174.0, 173.8, 140.9, 140.5, 138.0, 131.0, 128.9, 128.2, 127.5, 127.4, 127.2, 60.6, 60.3, 51.7, 37.8, 34.2, 28.7, 25.9. TOF HRMS: m/z calcd for $C_{23}H_{24}O_4$ [M+H]+: 365.1753; found: 365.1737.

*4.1.5.2. Compound **10b***

This compound was prepared by using the general procedure for Suzuki reactions with compound **10b** to give compound **10b** as a white solid (26 mg, 47% yield). mp 113.2-114.2 °C. Rf 0.74 (30% EtOAc/Hex). ^{1}H NMR ($CDCl_3$) 400 MHz: δ 7.40 (d, J = 8.1 Hz, 2H), 7.08 (d, J = 8.2 Hz, 2H), 6.93 (s, 2H), 5.63–5.51 (m, 2H), 4.65–4.53 (m, 1H), 4.52–4.42 (m, 1H), 4.03 (dt, J = 11.1, 4.2 Hz, 1H), 3.90 (dt, J = 11.1, 4.1 Hz, 1H), 3.65 (dd, J = 12.5, 2.8 Hz, 1H), 2.82 (ddd, J = 12.9, 12.9, 7.9 Hz, 1H), 2.47–2.30 (m, 5H), 2.32 (s, 3H), 2.11–2.02 (m, 2H), 1.98 (s, 6H). ^{13}C NMR ($CDCl_3$) 100 MHz: δ 174.3, 173.8, 140.2, 138.7, 137.1, 136.7, 136.2, 130.9, 129.7, 129.0, 128.2, 127.7, 60.5, 60.3, 51.7, 37.9, 34.2, 28.7, 25.9, 21.1, 20.9. TOF HRMS: m/z calcd for $C_{26}H_{30}O_4$ [M+H]+: 407.2222; found: 407.2189.

*4.1.5.3. Compound **10c***

This compound was prepared by using the general procedure for Suzuki reactions with compound **10c** to give compound **10c** as a white solid (27 mg, 52% yield). mp 151.6-152.3. °C Rf 0.25 (30% EtOAc/Hex). ^{1}H NMR ($CDCl_3$) 300 MHz: δ 7.51 (d, J = 8.0 Hz, 2H), 7.42 (d, J = 8.0 Hz, 2H), 7.32–7.24 (m, 1H), 7.15–7.04 (m, 2H), 6.84 (dd, J = 8.0, 2.5 Hz, 1H), 5.95–5.70 (br, 1H), 5.63–5.48 (m, 2H), 4.61–4.51 (m, 1H), 4.51–4.41 (m, 1H), 4.03 (dt, J = 11.2, 4.2 Hz, 1H), 3.87 (dt, J = 11.2, 4.1 Hz, 1H), 3.63 (dd, J = 12.5, 2.9 Hz, 1H), 2.79 (ddd, J = 12.9, 12.9, 7.8 Hz, 1H), 2.51–2.22 (m, 5H), 2.08–2.00 (m, 2H). ^{13}C NMR ($CDCl_3$) 75 MHz: δ 174.4, 174.2, 156.4, 142.5, 140.1, 138.0, 131.0, 130.1, 128.9, 128.2, 127.4, 119.5, 114.5, 114.1, 60.7, 60.4, 51.6, 37.8, 34.2, 28.7, 25.8. TOF HRMS: m/z calcd for $C_{23}H_{24}O_5$ [M+H]+: 381.1702; found: 381.1680.

*4.1.5.4. Compound **10d***

This compound was prepared by using the general procedure for Suzuki reactions with compound **9d** to give compound **10d** as a white solid (34 mg, 61% yield). mp 117.2-117.9 °C. Rf 0.51 (30% EtOAc/Hex). ^{1}H NMR ($CDCl_3$) 300 MHz: δ 7.51 (d, J = 8.0 Hz, 2H), 7.39 (d, J = 8.0 Hz, 2H), 7.29–7.22 (m, 1H), 6.89 (d, J = 7.7 Hz, 1H), 6.87 (s, 1H), 6.73-6.70 (m, 1H), 5.61–5.45 (m, 2H), 4.57–4.48 (m, 1H), 4.46–4.37 (m, 1H), 3.98 (dt, J = 11.2, 4.2 Hz, 1H), 3.82 (dt, J = 11.2, 4.1 Hz, 1H), 3.61 (dd, J = 12.5, 2.8 Hz, 1H), 2.96 (s, 6H), 2.77 (ddd, J = 12.9, 12.9, 7.8 Hz, 1H), 2.43–2.25 (m, 5H), 2.04–1.96 (m, 2H). ^{13}C NMR ($CDCl_3$) 75 MHz: δ 174.1, 173.8, 150.9, 142.0, 141.5, 137.8, 131.01, 129.6, 129.0, 128.0, 127.7, 116.0, 111.9, 111.7, 60.6, 60.3, 51.7, 40.9, 37.8, 34.2, 28.7, 25.9. TOF HRMS: m/z calcd for $C_{25}H_{29}NO_4$ [M+H]+: 408.2175; found: 408.2155.

*4.1.5.5. Compound **10e***

This compound was prepared by using the general procedure for Suzuki reactions with compound **9e** to give compound **10e** as a white solid (41 mg, 83% yield). mp 132.6-133.5 °C. Rf 0.36 (50% EtOAc/Hex). ^{1}H NMR ($CDCl_3$) 400 MHz: δ 8.82 (s, 1H), 8.57 (s, 1H), 7.83 (d, J = 7.9 Hz, 1H), 7.50 (q, J = 8.0 Hz, 4H), 7.38–7.28 (m, 1H), 5.65–5.46 (m, 2H), 4.54 (dt, J = 10.7, 7.4 Hz, 1H), 4.44 (dt, J = 15.0, 7.8 Hz, 1H), 4.04–4.00 (m, 1H), 3.88–3.83 (m, 1H), 3.65 (dd, J = 12.4, 2.8 Hz, 1H), 2.79 (ddd, J = 13.0, 13.0, 8.1 Hz, 1H), 2.45–2.27 (m, 5H), 2.06–2.00 (m, 2H). ^{13}C NMR ($CDCl_3$) 100 MHz: δ 173.9, 173.7, 148.6, 148.4, 138.9, 51.6, 37.8, 34.1, 28.6, 25.9. TOF HRMS: m/z calcd for $C_{22}H_{23}NO_4$ [M+H]+: 366.1705; found: 366.1694.

*4.1.5.6. Compound **10f***

This compound was prepared by using the general procedure for Suzuki reactions with compound **9f** to give compound **10f** as a white solid (28 mg, 56% yield). mp 144.3-145.2 °C. Rf 0.61 (pure EtOAc). ^{1}H NMR ($CDCl_3$) 300 MHz: δ 8.64 (s, 2H), 7.59 (d, J = 8.3 Hz, 2H), 7.53–7.43 (m, 4H), 5.64–5.48 (m, 2H), 4.55 (ddd, J = 11.0, 8.2, 6.5 Hz, 1H), 4.45 (ddd, J = 11.2, 8.2, 6.5 Hz, 1H), 4.02 (dt, J = 11.2, 4.2 Hz, 1H), 3.86 (dt, J = 11.2, 4.1 Hz, 1H), 3.66 (dd, J = 12.4, 2.9 Hz, 1H), 2.80 (ddd, J = 13.0, 13.0, 7.9 Hz, 1H), 2.48–2.24 (m, 5H), 2.08–2.00 (m, 2H). ^{13}C NMR ($CDCl_3$) 75 MHz: δ 173.8, 173.7, 150.4, 147.9, 140.0, 137.4, 131.3, 128.6, 127.4, 121.6, 60.7, 60.3, 51.7, 37.8, 34.1, 28.6, 25.9. TOF HRMS: m/z calcd for $C_{22}H_{23}NO_4$ [M+H]+: 366.1705; found: 366.1700.

*4.1.5.7. Compound **10g***

This compound was prepared by using the general procedure for Suzuki reactions with compound **9g** to give compound **10g** as a white solid (46 mg, 93% yield). mp 145.7-146.6 °C. Rf 0.68 (75% EtOAc/Hex). ^{1}H NMR ($CDCl_3$) 300 MHz: δ 9.18 (s, 1H), 8.91 (s, 2H), 7.53 (s, 4H), 5.63–5.47 (m, 2H), 4.58–4.50 (m, 1H), 4.48-4.40 (m, 1H), 4.02 (dt, J = 11.2, 4.2 Hz, 1H), 3.86 (dt, J = 11.2, 4.1 Hz, 1H), 3.66 (dd, J = 12.4, 2.9 Hz, 1H), 2.79 (ddd, J = 12.9, 12.9, 8.0 Hz, 1H), 2.46–2.28 (m, 5H), 2.08–2.00 (m, 2H). ^{13}C NMR ($CDCl_3$) 75 MHz: δ 173.7, 173.6, 157.6, 154.9, 140.0, 134.0, 133.5, 131.3, 128.9, 128.5, 127.3, 60.9, 60.3, 51.7, 37.8, 34.1, 28.6, 25.9. TOF HRMS: m/z calcd for $C_{21}H_{22}N_2O_4$ [M+H]+: 367.1658; found: 367.1663.

*4.1.5.8. Compound **10h***

This compound was prepared by using the general procedure for Suzuki reactions with compound **9h** to give compound **10h** as a white solid (57 mg, 98% yield). mp 114.3-114.7 °C. Rf 0.36 (30% EtOAc/Hex). ^{1}H NMR ($CDCl_3$) 400 MHz: δ 7.56 (d, J = 8.4 Hz, 2H), 7.47 (d, J = 8.3 Hz, 2H), 6.92 (s, 1H), 5.65–5.48 (m, 2H), 4.55 (ddd, J = 11.1, 8.5, 6.7 Hz, 1H), 4.45 (ddd, J = 11.2, 8.2, 6.5 Hz, 1H), 4.08 (s, 6H), 4.02 (dt, J = 11.2, 4.1 Hz, 1H), 3.86 (dt, J = 11.2, 4.1 Hz, 1H), 3.65 (dd, J = 12.4, 2.9 Hz, 1H), 2.79 (ddd, J = 13.0, 13.0, 8.3 Hz, 1H), 2.48–2.27 (m, 5H), 2.10–1.99 (m, 2H). ^{13}C NMR ($CDCl_3$) 75 MHz: δ 173.7, 162.7, 159.5, 140.2, 133.7, 132.6, 131.2, 129.3, 128.6, 128.0, 119.1, 60.7, 60.2, 54.9, 54.6, 51.7, 37.7, 34.1, 28.6, 25.8. TOF HRMS: m/z calcd for $C_{23}H_{26}N_2O_4$ [M+H]+: 427.1869; found: 427.1882.

*4.1.5.9. Compound **10i***

This compound was prepared by using the general procedure for Suzuki reactions with compound **9i** to give compound **10i** as a white solid (34 mg, 61% yield). mp 150.7-151.3 °C. Rf 0.58 (30% EtOAc/Hex). ^{1}H NMR ($CDCl_3$) 400 MHz: δ 8.29 (s, 1H), 7.66 (d, J = 8.2 Hz, 2H), 7.48 (d, J = 8.3 Hz, 2H), 7.39 (dt, J = 8.2, 1.0 Hz, 1H), 7.27–7.23 (m, 2H), 7.17 (dd, J = 7.3, 1.0 Hz, 1H), 6.78–6.66 (m, 1H), 5.65-5.53 (m, 2H), 4.65–4.53 (m, 1H), 4.53–4.41 (m, 1H), 4.04 (dt, J = 11.2, 4.2 Hz, 1H), 3.89 (dt, J = 11.2, 4.1 Hz, 1H), 3.69 (dd, J = 12.5, 2.9 Hz, 1H), 2.85 (ddd, J = 12.8, 12.8, 7.9 Hz, 1H), 2.47–2.28 (m, 5H), 2.16–1.97 (m, 2H). ^{13}C NMR ($CDCl_3$) 100 MHz: δ 174.2, 173.8, 140.5, 137.4, 136.4, 134.0, 130.9, 129.0, 129.0, 127.9, 126.2, 124.6, 122.3, 119.7, 110.4, 102.1, 60.6, 60.4, 51.7, 37.8, 34.2, 28.7, 25.9. TOF HRMS: m/z calcd for $C_{25}H_{25}NO_4$ [M+H]+: 404.1862; found: 404.1832.

*4.1.5.10. Compound **10j***

for Suzuki reactions with compound **9j** to give compound **10j** as a white solid (38 mg, 73% yield). mp 124.8-125.8 °C. Rf 0.44 (30% EtOAc/Hex). ^{1}H NMR ($CDCl_3$) 300 MHz: δ 7.44 (d, J = 8.2 Hz, 2H), 7.20 (d, J = 8.2 Hz, 2H), 5.72–5.45 (m, 2H), 4.55 (ddd, J = 11.1, 8.3, 6.6 Hz, 1H), 4.45 (ddd, J = 11.2, 8.3, 6.6 Hz, 1H), 4.02 (dt, J = 11.2, 4.2 Hz, 1H), 3.87 (dt, J = 11.2, 4.1 Hz, 1H), 3.64 (dd, J = 12.4, 2.8 Hz, 1H), 2.79 (ddd, J = 12.9, 12.9, 7.9 Hz, 1H), 2.47–2.28 (m, 5H), 2.38 (s, 3H), 2.25 (s, 3H), 2.10–2.00 (m, 2H). ^{13}C NMR ($CDCl_3$) 75 MHz: δ 174.0, 173.7, 165.3, 158.8, 138.2, 131.2, 129.7, 129.4, 128.7, 128.2, 116.4, 60.7, 60.3, 51.7, 37.8, 34.2, 28.6, 25.9, 11.7, 11.0. TOF HRMS: m/z calcd for $C_{22}H_{25}NO_5$ [M+H]+: 384.1811; found: 384.1831.

*4.1.5.11. Compound **10k***

This compound was prepared by using the general procedure for Suzuki reactions with compound **9k** to give compound **10k** as a white solid (46 mg, 76% yield). mp 145.4-146.2 °C. Rf 0.36 (30% EtOAc/Hex). ^{1}H NMR ($CDCl_3$) 400 MHz: δ 7.80 (s, 1H), 7.59 (s, 1H), 7.47–7.16 (m, 9H), 5.61–5.49 (m, 2H), 5.33 (s, 2H), 4.58-4.51 (m, 1H), 4.47–4.40 (m, 1H), 4.04–4.00 (m, 1H), 3.86–3.81 (m, 1H), 3.59 (dd, J = 13.6, 2.8 Hz, 1H), 2.77 (ddd, J = 13.0, 13.0, 8.0 Hz, 1H), 2.45–2.26 (m, 5H), 2.11–1.94 (m, 2H). ^{13}C NMR ($CDCl_3$) 75 MHz: δ 174.0, 173.7, 137.1, 137.1, 136.5, 131.9, 131.0, 129.0, 128.9, 128.2, 127.8, 126.3, 125.8, 123.2, 60.6, 60.3, 56.4, 51.6, 37.8, 34.2, 28.6, 25.9. TOF HRMS: m/z calcd for $C_{27}H_{28}NO_4$ [M+H]+: 445.2127; found: 445.2128.

4.2. Principal Component Analysis

The procedure for principal component analysis (PCA) used was the method used by Derek Tan and co-workers with minor modifications.[23] Specifications on the process of defining Chemical Field Terms in Instant JChem[28] as integers or decimal numbers can be found in the Supplementary data. This was a key step for obtaining any values that were not whole numbers and was especially true for values that were less than 1 such as Fsp^3, which would be returned as 0 if the specification was not made thus throwing off the entire calculation. In addition to this loading plots were generated using Excel. These plots were generated from PC1-PC3 coefficients of each parameter for each of the three PCA plots. Once the loading plots were made, the data labels were added. These plots were much clearer and easier for facile determination of parameter importance.

4.3. Cell proliferation assay[20,21]

ASZ cells were plated onto 96-well tissue culture plates and allowed to attach and grow for 24 h. Test compounds dissolved in DMSO were added at varying concentrations to experimental cultures at 1% DMSO final concentration. Cultures were then incubated for another 72 h. Controls, treated only with DMSO, were incubated in parallel to the test wells. Then, an MTS/PMS (20:1) solution was added to each well and the mixture incubated for 3 hours at 37 °C. Following incubation, absorbance was measured by spectrophotometry at 490 nm using a Biotek Synergy H1 Hybrid Reader. Reported values are the mean of two separate runs (with errors shown), where each run was conducted in triplicate. Absorbance data was normalized using the DMSO control values after background subtraction of the media-only wells. The percentage cell viability values were analyzed in GraphPad Prism to provide a GI_{50} value for cell viability through non-linear regression analysis. The GI_{50} values (Table 1) are average ± standard error mean (SEM), calculated using GraphPad Prism. The graphs (Fig. S1) are representative graphs of the data from two runs each performed in triplicate.

Conflicts of interest

The authors declare that there are no conflicts of interest.

Acknowledgments

R. McLean acknowledges partial support from the UConn Office of Undergraduate Research. C. McGeough was supported in part by National Science Foundation Research Experience for Undergraduates Grant CHE-1062946.

Appendix A. Supplementary data

Supplementary data associated with this publication can be found online at xxxxx.

References

1 Yudin AK. *Chem. Sci.* 2015; 6: 30-49.

2 Whitty A, Viarengo LA, Zhong M. *Org. Biomol. Chem.* 2017; 15: 7729-7735.

3 Larsen EM, Wilson MR, Taylor RE. *Nat. Prod. Rep.* 2015; 32: 1183-1206.

4 Driggers EM, Hale SP, Lee J, Terret NK. *Nat. Rev. Drug. Discov.* 2008; 7: 608-624

5 Villar EA, Beglov D, Chennamudhavuni S. Porco JA, Kozakov D, Vajda S, Whitty A. *Nat. Chem. Biol.* 2014; 10: 723-731.

6 Whitty A, Zhong M, Viarengo LA, Beglov D, Hall DR, Vajda S. *Drug Discov. Today* 2016; 21: 712-717.

7 Rutledge KM, Hamlin TA, Baldisseri D, Peczuh MW. *Chem. Asian J.* 2017; *12*: 2623-2633.

8 Magpusao AN, Rutledge KM, Hamlin TA, Lawrence J-M, Mercado BQ, Leadbeater NE, Peczuh MW. *Chem. Eur. J.* 2016; *22*: 6001-6011.

9 Magpusao AN, Rutledge K, Mercado B, Peczuh MW. *Org. Biomol. Chem.* 2015; 13: 5086-5089.

10 Ma J, Vannam R, Terwilliger DW, Peczuh MW. *Tetrahedron Lett.* 2014; 55: 4255-4259.

11 Ma J, Peczuh MW. *J. Org. Chem.* 2013; 78: 7414-7422.

12 Magpusao AN, Desmond RT, Billings KJ, Fenteany G, Peczuh MW. *Bioorg. Med. Chem. Lett.* 2010; 20: 5472-5476.

13 Oskarsson T, Nagorny P, Krauss IJ, Perez L, Mandal M, Yang G, Ouerfelli O, Xiao D, Moore MAS, Massague J, Danishefsky SJ. *J. Am. Chem. Soc.* 2010; 132: 3224-3228.

14 Metaferia BB, Chen L, Baker HL, Huang X-Y, Bewley CA. *J. Am. Chem. Soc.* 2007; 129: 2434-2435.

15 Tyagi M, Begnini F, Poongavanam V, Doak BC, Kihlberg J.

Chem. Eur. J. 2020; 26: 49-88

16 Chen Q-H, Rao PNP, Knaus EE. *Bioorg. Med. Chem*. 2005; 13: 4694–4703.

17 Pour M, Spulak M, Buchta V, Kubanova P, Voprsalova M, Wsol V, Fakova H, Koudelka P, Pourova H, Schiller R. *J. Med. Chem.* 2001; 44: 2701-2706

18 Kudo N, Perseghini M, Fu G. *Angew. Chem*. 2006; 118: 1304–1306.

19 Kuete, V, Karaosmanoğlu, O, Sivas, H. Chapter 10 - Anticancer Activities of African Medicinal Spices and Vegetables. In *Medicinal Spices and Vegetables from Africa*; Kuete, V, Ed. Academic Press, 2017; pp 271–297

20 Buttke TM, McCubrey JA, Owen TC. *J. Immunol. Methods* 1993; 157: 233–240.

21 Cory AH, Owen TC, Barltrop JA, Cory JG. *Cancer Commun.* 1991; 3: 207–212.

22 Kopp F, Stratton CF, Akella LB, Tan DS. *Nat. Chem. Biol.* 2012; 8: 358–365.

23 Wenderski TA, Stratton CF, Bauer RA, Kopp F, Tan DS. *Methods Mol. Biol.* 2015; 1263: 225–242.

24 The PC3 vs PC2 plot is very similar to the PC1 vs PC2 plot. See the Supplementary data.

25 Harvey, A. Natural Products in Drug Discovery. *Drug Discovery Today* 2008; 13:894–901.

26 Over B, Matsson P, Tyrchan, C, Artusson P, Doak BC, Foley MA, Hilgendorf C, Johnston SE, Lee MD, Lewis RJ, McCarren P, Muncipinto G, Norinder U, Perry MWD, Duvall JR, Kihlberg J. *Nat. Chem. Biol.* 2016, 12: 1065-1074.

27 Ling LL, Schneider T, Peoples AJ, Spoering AL, Engels I, Conlon BP, Mueller A, Schäberle TF, Hughes DE, Epstein S, Jones M, Lazarides L, Steadman VA, Cohen DR, Felix CR, Fetterman KA, Millett WP, Nitti AG, Zullo AM, Chen C, Lewis K. *Nature* 2015; 517: 455–459.

28 Instant JChem was used for structure database management, search and prediction, Instant JChem 18.8.0, 2018, ChemAxon (http://www.chemaxon.com)